International Journal of Fatigue 45 (2012) 39–47

Contents lists available at SciVerse ScienceDirect

International Journal of Fatigue

journal homepage: www.elsevier.com/locate/ijfatigue

Fast time-scale average for a mesoscopic high cycle fatigue criterion

Stefano Bosia [a,b,*], Andrei Constantinescu [a]

[a] Laboratoire de Mécanique des Solides, CNRS – Ecole Polytechnique, 91128 Palaiseau cedex, France
[b] Dipartimento di Matematica "F.Brioschi", Politecnico di Milano, Piazza Leonardo da Vinci 32, 20133 Milano, Italy

ARTICLE INFO

Article history:
Received 28 March 2012
Received in revised form 13 June 2012
Accepted 15 June 2012
Available online 28 June 2012

Keywords:
Multi-axial fatigue
Dang Van fatigue criterion
High-cycle fatigue
Dynamical systems
Fasttime scale average

ABSTRACT

The paper discusses the lifetime prediction of structures in high-cycle fatigue based on the two-scale fatigue criteria of Dang Van type and several of its extensions in finite lifetime regime. The main assumptions for this criteria are (i) the material is polycrystalline and undergoes localised plasticity in one of the misoriented grains and (ii) crack initiation arises as a consequence of cumulated plasticity in this grain.

The novelty of the presented approach is twofold. On the one hand a generalisation of mesoscopic plasticity model is presented, on the other a fast time scale average is introduced for tracking the cyclic material behaviour and the subsequent evolution of damage. The tracking method is based on the split between a quick quasi-periodic response of the system to the cyclic load and a slow evolution of the internal hardening and damage parameters of the material at the mesoscopic scale. The proposed method can be extended to a large class of local material behaviours involving not only plasticity, but also crack and damage evolution.

The paper proposes a simplified plasticity-based model for the mesoscopic material behaviour and presents a comparison between predicted and experimental lifetimes. The results are discussed in terms of prediction capabilities and also in terms of the identification procedure of parameters of the mesoscopic model.

1. Introduction

A series of fatigue prediction models for the cyclic behaviour of structures is based on multiscale analysis. These try to bridge the gap between the fine evolution of the defects at the scale of the microstructure and the load transmitted from the macroscopic scale of the structure. The analysis usually involves homogenisation techniques for the smaller scales and is based on the concept of shakedown. This amounts to characterising the cyclic behaviour through an asymptotic limit cycle, which is either plastic or elastic denoting respectively presence or absence of dissipation.

This paper addresses the question of finite lifetime in the *high cycle fatigue* (HCF) regime for metallic polycristalline materials. Within HCF, it is common to assume that the structure is in elastic shakedown at the macroscopic scale but undergoes elastic or plastic shakedown at the mesoscale (i.e. scale of the grains) for infinite or finite lifetime respectively. In the case of finite lifetime, we will refer to the time to failure of the material with the expression *lifetime*.

In this general framework, the initial fatigue criterion proposed by Dang Van (DVK) in [6] (and extended in [21–25]) has been highly successful in predicting the infinite lifetime of structures. The DVK fatigue criterium decides whether or not the structure will have an infinite lifetime by considering the shakedown limit of the slip system in the different grains. This approach was expressed later in a more general term through the Melan–Koiter shakedown theorem (see [7,19] and references therein). The hydrostatic stress is considered in order to account for the local heterogenous structure. This has only recently been justified using a precise homogenisation procedure [3,15].

In order to give quantitative estimates of the lifetime, several extensions of the DVK criterion have been proposed. Among others we recall the models of Morel [16,17] and of Maitournam et al. [11,13]. In the first case, a simple mesoscopic plastic model is introduced. The evolution of the cumulated plastic strain up to final failure at the mesoscopic level is evaluated to effectively predict lifetime under cyclic and variable loading. The second model differs from this approach by (i) proposing a mesoscopic plastic model depending on the hydrostatic stress component to account for the damage process; (ii) estimating the plastic shakedown cycle at the mesoscopic scale using a classical fatigue criterion based on the range of plastic strain.

The extension discussed in this paper is constructed under similar assumptions to those of Morel's model [16,17]. However, it is grounded on a generalisation of the mesoscopic plasticity model and introduces a new fast time scale average for tracking the cyclic

* Corresponding author at: Laboratoire de Mécanique des Solides, CNRS – Ecole Polytechnique, 91128 Palaiseau cedex, France.
E-mail addresses: bosia@lms.polytechnique.fr (S. Bosia), constant@lms.polytechnique.fr (A. Constantinescu).

0142-1123/$ - see front matter © 2012 Elsevier Ltd. All rights reserved.
http://dx.doi.org/10.1016/j.ijfatigue.2012.06.015

Nomenclature

$\mathbf{A}$	localisation tensor	T_a	amplitude of the mesoscopic resolved shear stress
$\mathbf{b}$	mesoscopic kinematical hardening vector	t_{-1}	fatigue limit under fully reversed torsion
$\mathbf{C}$	macroscopic elasticity tensor	$\boldsymbol{\epsilon}$	mesoscopic strain
$\mathbf{c}$	mesoscopic elasticity tensor	$\boldsymbol{\epsilon}^p$	mesoscopic plastic strain
c	kinematic hardening parameter	$\boldsymbol{\epsilon}^p_d$	deviatoric part of the mesoscopic plastic strain
$\mathbf{E}$	macroscopic strain	$\boldsymbol{\epsilon}^{pc}$	cumulated mesoscopic plastic strain
$\mathbf{E}^p$	macroscopic plastic strain	Γ	cumulated plastic mesostrain
f_{-1}	fatigue limit under fully reversed tension compression	$\boldsymbol{\gamma}^p$	mesoscopic shear plastic strain
$\mathbf{L}$	macroscopic compliance tensor	λ, μ	macroscopic Lamè parameters
$\mathbf{l}$	mesoscopic compliance tensor	$\boldsymbol{\Sigma}$	macroscopic stress
p	mesoscopic hydrostatic stress	$\boldsymbol{\sigma}$	mesoscopic stress
$S^H_{\max}$	maximal hydrostatic stress during one loading cycle	σ^m_{xx}	mean normal stress in the x direction
$\mathbf{T}$	macroscopic resolved shear stress	σ^a_{xx}	amplitude of the normal stress in the x direction
ΔT	amplitude of the macroscopic resolved shear stress	$\boldsymbol{\tau}$	mesoscopic resolved shear stress
ΔT_0	amplitude of the macroscopic resolved shear stress on the critical plane for limit loading	τ_y	shear yield limit of a crystal
		τ^a_{xy}	amplitude of xy shear component of stress tensor

material behaviour and the subsequent evolution of damage. This separation of time scales is justified by the great number of cycles usually considered in HCF experiments (10^4–10^7 cycles). The cyclic material behaviour can be viewed as the succession of (a) a short hardening (or softening) transient up to a saturation point, (b) a long phase close to a stable cycle and (c) a final brief softening predicting failure. The long transient observed in the second phase above can be described through the theory of dynamical systems as the presence of a saddle-node ghost (see [26] and references therein) and is therefore amenable to precise analytical study.

The paper starts with a short presentation of the two scale model used in the HCF theory. We then introduce three different constitutive laws and the relative techniques to compute lifetimes. In particular we discuss: (i) Maitournam's et al., (ii) Morel's, and (iii) the present model. Sections 2 and 3 discuss the main analytical tools from dynamical systems theory, namely separation of timescales and saddle-node ghost estimates. In Section 4 the identification method for the parameters of the model is detailed. Finally Sections 5 and 6 present the prediction capabilities for experiments extracted from literature and conclusions. An appendix completes the presentation with an extended computation of the lifetime using the saddle-node ghost estimates.

2. The models at the mesoscopic scale

In the framework of HCF for metallic polycristalline materials, one can assume that only a few grains of the material undergo plastic deformations whilst most of the material remains elastic. We can therefore consider the material point at the macroscopic scale as a representative elementary volume (REV) at the mesoscopic scale. This volume is a non-homogeneous medium, which can be assimilated under the given assumptions to an elastic matrix and an elasto-plastic inclusion (grain).

The loading of the REV, i.e. macroscopic stresses $\boldsymbol{\Sigma}$ and strains $\mathbf{E}$, can be computed in the framework of the standard continuum theory (macroscale) and will be considered as given in this work. In order to evaluate the mesoscopic state, i.e. mesoscopic stresses $\boldsymbol{\sigma}$ and strains $\boldsymbol{\epsilon}$, several homogenisation techniques have been considered in the literature. The models of Bui, Lin–Taylor, Kröner–Budansky–Wu and Sachs have been described in relation with the DVK fatigue criterion for example in [2,7,11,13].

Without restraining the generality, we shall adopt here the Lin–Taylor's homogenisation scheme, which is based on the equality of macroscopic and mesoscopic strain:

$$\boldsymbol{\epsilon} = \mathbf{E}.$$

As pointed out by Dang Van (see [5,7] and references therein), when dealing with the description of HCF, Lin–Taylor's approximation is particularly effective as it permits to accept the existence of mesoscopic plastic strain and residual stress fields. Therefore, we will limit the presentation to this particular case.

Let us denote by $\mathbf{C}$ and $\mathbf{c}$ the macroscopic and mesoscopic elasticity tensor, and by $\mathbf{L}$ and $\mathbf{l}$ the macroscopic and mesoscopic compliance tensors. For completeness reasons we also introduce both the mesoscopic plastic strain tensor $\boldsymbol{\epsilon}^p$ and the macroscopic plastic strain tensor $\mathbf{E}^p$. However, as in HCF the structure is in elastic shakedown at the macroscopic level, it follows that (see Fig. 1)

$$\mathbf{E}^p = \mathbf{0}.$$

With this notation the main assumptions of Lin–Taylor's model are equality of macroscopic and mesoscopic elasticity tensors and equality of the respective strains:

$$\mathbf{C} = \mathbf{c} \qquad \mathbf{E} = \boldsymbol{\epsilon}.$$

Assuming that the behaviour at the macroscopic scale is purely elastic, from the expressions of the elastic Hooke's law at the macroscopic and mesoscopic scale we deduce

$$\boldsymbol{\sigma} = \mathbf{A}\boldsymbol{\Sigma} - \mathbf{AC}(\boldsymbol{\epsilon}^{\mathbf{p}} - \mathbf{E}^{\mathbf{p}}) \tag{1}$$

where the fourth-order tensor $\mathbf{A}$ is the localisation tensor defined by

$$\mathbf{A} \doteq \mathbf{c} : \mathbf{L}.$$

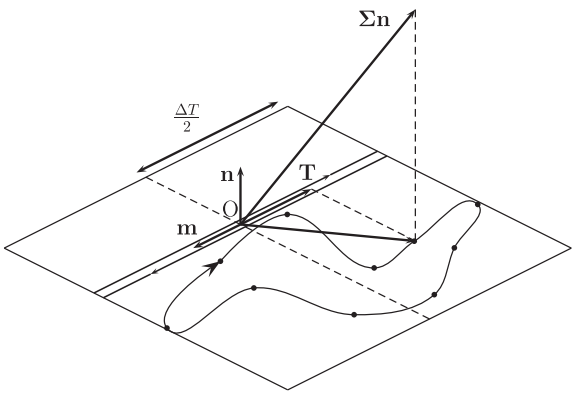

Fig. 1. Path of the macroscopic shear stress on the material plane identified by $\mathbf{n}$ at the point O and the corresponding path of the macroscopic resolved shear stress $\mathbf{T}$ acting on a glide direction.

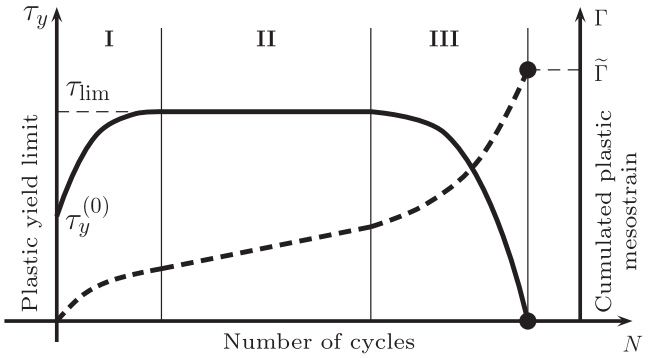

Fig. 2. Scheme for the evolution of the yield limit (continuous line) and of the damage (cumulated plastic mesostrain—dashed line) in function of the number of cycles. The material behaviour involves a hardening phase (I), a saturation phase (II) and a final softening (III). Recall that under periodic loading, number of cycles and time are equivalent up to a constant factor.

The next step in the modelling is the introduction of a suitable material behaviour at the mesoscopic scale in order to take into account fatigue. The experimental evidence leads to consider a three-phase model involving an initial hardening (or softening) phase, followed by a stable saturation phase and a final softening [18,16,17] as schematically displayed in Fig. 2. Under these assumptions, failure corresponds to vanishing mesoscopic yield limit. As the yield limit is directly related to the cumulated plastic mesostrain, denoted by Γ hereafter (see Eq. (8) below), one can also express failure as limit of cumulated plastic mesostrain $\widetilde{\Gamma}$:

$$\Gamma = \widetilde{\Gamma}.$$

We recall that cumulated plastic mesostrain is a monotonic increasing function of the number of loading cycles the system has endured and that the plastic models considered here are rate independent. Therefore, it can be appropriately chosen as an independent variable to represent the evolution of the yield limit instead of time or of number of cycles. This approach will be followed in the present formulation (see also Fig. 3 later on).

Assuming further that only one glide plane is active for any plastically deforming inclusion of the medium (grain), it has been shown in [22] that relation (1) for a perfectly elastic matrix can be reduced to

$$\boldsymbol{\tau} = \mathbf{T} - \mu\gamma^p\mathbf{m} \tag{2}$$

where $\mathbf{T}$ and $\boldsymbol{\tau}$ are the macroscopic and mesoscopic resolved shear stresses acting along the slip direction $\mathbf{m}$ of the plane identified by its normal $\mathbf{n}$ and μ is the shear modulus of the λ, μ Lamè constants [4,9]. Explicitly the later are defined by:

$$\mathbf{T} = (\mathbf{m}\otimes\mathbf{n} : \boldsymbol{\Sigma})\mathbf{m}$$
$$\boldsymbol{\tau} = (\mathbf{m}\otimes\mathbf{n} : \boldsymbol{\sigma})\mathbf{m}.$$

The mesoscopic plastic model is now determined by defining:

- the yield function $f(\boldsymbol{\tau}, \mathbf{b}, \tau_{\mathbf{y}})$
- the hardening rule, assumed to be in the general form

$$\dot{\tau_y} = g(\Gamma)\dot{\Gamma} \tag{3}$$

which implies by integration that

$$\tau_y = G(\Gamma) \tag{4}$$

where G is a suitable primitive function of g.

If this plastic model is brought into the three-phase description of cyclic material behaviour previously introduced, one has to require G to be a concave function increasing when Γ is small and decreasing for larger values of the mesoscopic shear plastic strain. Moreover there will be a unique value for the cumulated plastic mesostrain denoted by $\widetilde{\Gamma}$ for which the following hold:

$$G(\widetilde{\Gamma}) = 0, \qquad G(\widetilde{\Gamma})' < 0. \tag{5}$$

In this terms, the *lifetime* defined as the failure of the REV, or equivalently as the initiation of a macroscopic crack is defined as the unique time instant $\widetilde{t}$ for which

$$\Gamma(\widetilde{t}) = \widetilde{\Gamma}.$$

As a consequence of the definition of $\widetilde{\Gamma}$, one can equally express the lifetime by a vanishing plastic yield at the mesoscale (see (4)).

A large panel of choice for the definition of the yield function f and for the evolution of the yield limit τ_y is possible. Among the different models proposed in the literature, we shall only recall the proposals of Maitournam et al. and the one of Morel.

2.1. Maitournam's model [13]

The proposal of this model is to consider a plastic material behaviour at the mesoscale with a dependence of the yield function not only on the deviatoric part of the stress but also on the hydrostatic part. A kinematic hardening under the assumptions of associative plasticity is also considered. The mesoscopic yield function can therefore be written as

$$f(\boldsymbol{\sigma}, \boldsymbol{\epsilon}_d^p, p) \doteq \sqrt{\frac{1}{2}(\boldsymbol{\sigma} - h\boldsymbol{\epsilon}_d^p) : (\boldsymbol{\sigma} - h\boldsymbol{\epsilon}_d^p)} - k(p)$$

with

$$k(p) = \beta - \alpha p(t) \qquad \text{or} \qquad k(p) = \begin{cases} \beta - \alpha p & \text{if } p \geqslant 0 \\ \beta - \gamma p & \text{if } p < 0 \end{cases}$$

and where p is the mesoscopic hydrostatic stress, $\boldsymbol{\epsilon}_d^p$ the deviatoric part of the mesoscopic plastic strain tensor and α, β, γ and h are suitable parameters.

The underlying hypothesis of this model consider that the mesostructure can be computed from the macroscopic structure. Fatigue will then be determined from the plastic shakedown cycle and from a phenomenological fatigue law linking lifetime and cumulated mesoscopic plastic strain ($\boldsymbol{\epsilon}^{pc}$):

$$N = g(\boldsymbol{\epsilon}^{pc}).$$

which is a Manson–Coffin type fatigue criterion.

2.2. Morel's model [16,17]

This model considers a complete description for the mesoscopic plastic yield limit as introduced above. Three sharply separated phases account for the hardening of the mesoscopic inclusion. The dependence of the yield limit on plastic strain is piece-wise linear (see Fig. 3). Moreover, the yield function is defined in terms of the resolved shear stress and has both isotropic and kinematic hardening terms:

$$f(\boldsymbol{\tau}, \mathbf{b}, \tau_y) = (\boldsymbol{\tau} - \mathbf{b}) \cdot (\boldsymbol{\tau} - \mathbf{b}) - \tau_{\mathbf{y}}^{\mathbf{2}}. \tag{6}$$

In this case, the three phase of the plastic inclusion are defined as:

$$\dot{\tau_y} = \begin{cases} g\dot{\Gamma} & \text{during hardening;} \\ 0 & \text{during the saturation phase;} \\ -h\dot{\Gamma} & \text{during softening;} \end{cases} \tag{7}$$
$$\dot{\mathbf{b}} = c\dot{\boldsymbol{\gamma}}^p$$

where $\boldsymbol{\gamma}^p$ is the mesoscopic shear plastic strain and Γ is the cumulated plastic mesostrain given by

$$\dot{\Gamma} \doteq \sqrt{\dot{\boldsymbol{\gamma}}^p \cdot \dot{\boldsymbol{\gamma}}^p}. \tag{8}$$

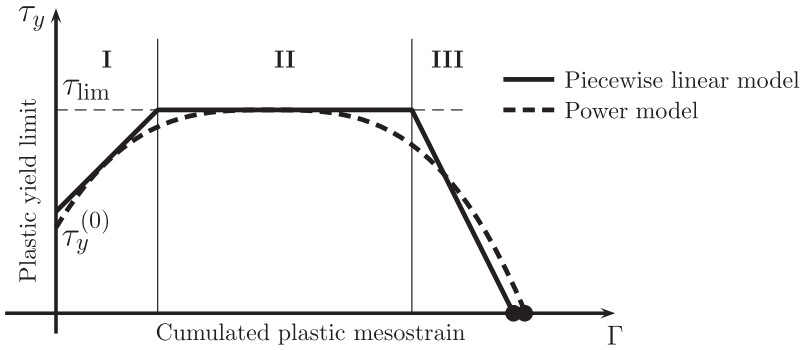

Fig. 3. The three-phase evolution of the plastic yield limit. Comparison between the piecewise linear model (Morel—continuous line) and the power model (dashed line).

2.3. Power law model

The model used in this work replaces the piecewise-linear dependence in the evolution of the yield limit with a power law. When compared with the model of Morel, one immediately notices the advantages arising from the piecewise-linear description. Indeed, in this latter case, for periodic macroscopic loadings it is possible to obtain explicitly the lifetime (see [16]). However, the hardening rule (7) is a rough approximation of the actual behaviour of materials, for which the sharp transitions between hardening and saturation regimes as well as from saturation to softening regimes are difficult to justify.

An alternative model is given by the following constitutive power law

$$G(\Gamma)\doteq\frac{\Delta T_0}{2}-\frac{|\Gamma-\Gamma_0|^{\alpha}}{\beta} \tag{9}$$

with $\alpha>1$, which naturally satisfies the constraints of concavity and monotonicity introduced above (see Fig. 3).

When compared with the piecewise linear model of Morel, one cannot hope to retrieve exact lifetime estimates for this model. However, as we shall see below, precise a priori analytical estimates can be derived in this setting under mild regularity assumption on the behaviour of the function G, which are satisfied by the power law (9). Before delving into the details of such estimates, we will derive a suitable approximation for the just introduced constitutive laws in the case of periodic loadings. In particular we now want to consider a time-average over each cycle of the loading.

3. Separation of time scales

In the regime of HCF we can distinguish between a quick quasi-periodic response of the system to the cyclic charge and a slow evolution of the inner parameter describing the hardening and damage of the material itself. This separation of time scales is justified by the great number of cycles usually considered in HCF experiments (10^4–10^7 cycles). It seems therefore sound to look for a slowly-varying approximation for this internal variable and for the cumulated plastic mesostrain Γ, by averaging out the periodic behaviour of the system. This process is also known as "time-homogenisation" (see [1,10]).

By differentiating the yield function (6) with respect to time we obtain:

$$\dot f=2(\boldsymbol{\tau}-\mathbf{b})\cdot\dot{\boldsymbol{\tau}}+\mathbf{2}(\mathbf{b}-\boldsymbol{\tau})\cdot\dot{\mathbf{b}}-\mathbf{2}\tau_{\mathbf{y}}\dot\tau_{\mathbf{y}}.$$

Since during plastic deformations the yield function f is constant ($f\equiv 0$), by recalling relation (2), we deduce

$$\dot T-\mu\dot\gamma^p-c\dot\gamma^p=g(\Gamma)\dot\Gamma$$

where we have set

$$\boldsymbol{\gamma}^p=\gamma^p\mathbf{m}.$$

From definition (8) we have

$$\dot\Gamma=|\dot\gamma^p|$$

and therefore

$$\dot\Gamma=\frac{|\dot T|}{g(\Gamma)+c+\mu},$$

which represents the evolution law for the cumulated plastic mesostrain during plastic deformations. Obviously Γ is constant during the elastic part of the loading so that we can deduce the following ordinary differential equation describing the evolution of the cumulated plastic mesostrain

$$\dot\Gamma=\begin{cases}\frac{|\dot T|}{g(\Gamma)+c+\mu} & \text{when } f=0,\\ 0 & \text{when } f<0.\end{cases} \tag{10}$$

We recall that the cumulated plastic mesostrain Γ is a nondecreasing function of time also if the resolved plastic mesostrain γ^p oscillates. Indeed, Γ accounts for all the plastic deformations the material has endured up to the current time.

We now want to simplify the evolution law (10) in the special case of cyclic loadings. By the above discussion it is easy to see that under a periodic loading of equivalent amplitude comparable to ΔT_0, the plastic mesostrain changes only slightly during one charge/discharge cycle. Therefore, the increase per cycle of the cumulated plastic mesostrain is small when compared with the variation of the mesoscopic strain. This justifies us stating that the evolution of cumulated plastic strain is slow with respect to the evolution of the mesoscopic strain. As a consequence, we can assume that Γ constant during each cycle.

By considering Γ as constant during one period of the forcing term, we can decouple the quick dynamic of the elasto-plastic response of the material to the external loading and the slow evolution of the internal damaging mechanism (i.e. the slow drift of Γ). We denote by ΔT the amplitude of the macroscopic resolved shear stress. In order to integrate (10) on a single cycle, we observe that during a complete unloading–loading phase from $-\Delta T/2$ to $\Delta T/2$, the mesoscopic inclusion will be in elastic regime ($f<0$) up to $T=-\Delta T/2+2\tau_y$. therefore, we obtain (see Fig. 4 and [17, Appendix A])

$$\int_{f=0}\dot T=\frac{\Delta T}{2}-\left(-\frac{\Delta T}{2}+2\tau_y\right)=\Delta T-2\tau_y.$$

By taking into account the second half of the loading cycle (i.e. the transition of T from $\Delta T/2$ to $-\Delta T/2$), and using this result in (10) we finally have

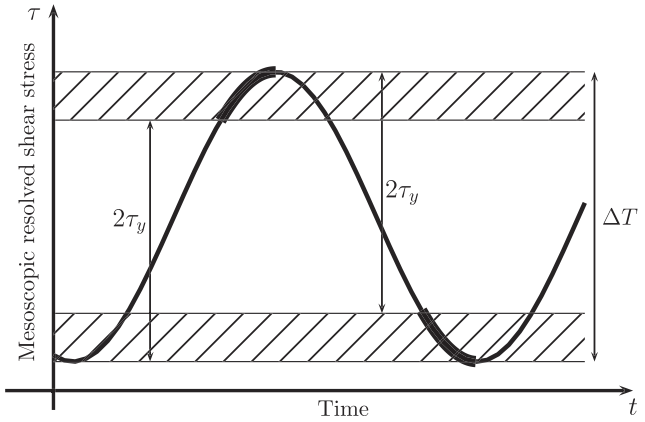

Fig. 4. Illustration of the relation between the periodic resolved plastic shear stress and the evolution of the cumulated plastic mesostrain. Notice that only the heavily thickened part of the loading cycle contributes to plastic deformations. The amplitude of the hatched regions has been emphasise for clarity of expositions.

$$\Delta_{\text{cycle}}\Gamma = \int_{\text{cycle}} \dot{\Gamma} = \frac{4}{\mu + c + g(\Gamma)}\left(\frac{\Delta T}{2} - \tau_y\right).$$

where $\Delta_{\text{cycle}}\Gamma$ represents the (small) change in Γ during a single complete loading cycle.

The behaviour of the simple system we are studying can therefore be reduced to a system of an ordinary differential equation and a difference equation

$$\begin{cases} \Delta_{\text{cycle}}\Gamma = \frac{4}{\mu+c+g(\Gamma)}\left(\frac{\Delta T}{2} - \tau_y(\Gamma)\right) \\ \dot{\tau_y} = g(\Gamma)\dot{\Gamma}. \end{cases}$$

If we consider an adimensionalized time period equal to 1 for the cycle forcing term $\Delta_{\text{cycle}}t = 1$ (i.e. if we measure time by the number of cycles of the periodic loading the system has undergone), we can average the evolution equation for the cumulated plastic mesostrain getting the following ordinary differential equation system

$$\begin{cases} \dot{\Gamma} \approx \frac{\Delta_{\text{cycle}}\Gamma}{\Delta_{\text{cycle}}t} = \frac{4}{\mu+c+g(\Gamma)}\left(\frac{\Delta T}{2} - \tau_y(\Gamma)\right) \\ \dot{\tau_y} = g(\Gamma)\dot{\Gamma}. \end{cases}$$

Recalling the integral relation (4) for the shear limit τ_y, we finally get the following ordinary differential equation describing the evolution of our medium

$$\dot{\Gamma} = \frac{4}{\mu + c + g(\Gamma)}\left(\frac{\Delta T}{2} - G(\Gamma)\right). \tag{11}$$

We recall that the proposed power law model for mesoscopic hardening is determined by 5 parameters. As we will discuss later, of these ΔT_0 can be directly identified by knowing the characteristic of the loading. Of the remaining parameters, α has a clear physical significance representing the "flatness" of the hardening law (see Fig. 5). This parameter with the other remaining three, namely Γ_0, β and the sum $\mu + c$ will be identified through a fitting procedure.

4. Lifetime estimates in HCF

In the discussion of the previous section no explicit reference to the analytic form of the constitutive relation $G(\Gamma)$ has been made. We now want to particularise the above results by choosing as constitutive hardening relation the power model (9) introduced above.

In this case, Eq. (11) exhibits a threshold behaviour controlled by the value of ΔT. If $\frac{\Delta T}{2}$ is smaller than $\frac{\Delta T_0}{2}$ (i.e. if it is smaller than the maximum value attained by $G(\Gamma)$), then the system will undergo elastic shakedown and be in an infinite endurance regime. If, otherwise, $\frac{\Delta T}{2}$ is above this value, then the material will eventually fail (i.e. $G(\Gamma) \to 0$).

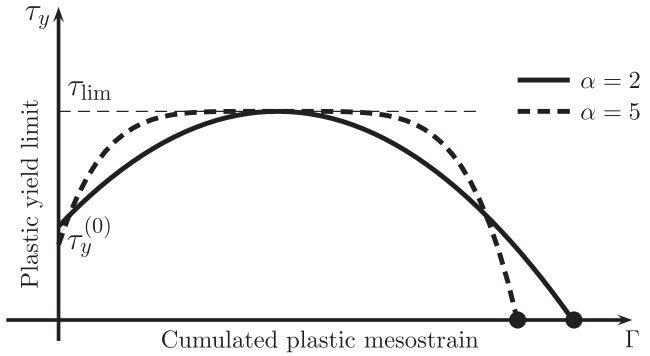

Fig. 5. The dependence of the mesoscopic hardening law on the "flatness" parameter α. Note that for larger αs (dashed line) the plateau is longer.

Due to the hypothesis of concavity and regularity on $G(\Gamma)$, for values of ΔT near the threshold value, the system will show a very long transient regime, which is proceeded and followed by two phases of faster evolution. The time span of this transient regime will constitute the fundamental element for our estimate of the lifetime of the material in HCF regime. Incidentally, we observe that this kind of estimates will essentially be unaffected by changes of the expression of $G(\Gamma)$ far away from its maximal value.

Starting from (9), we immediately deduce

$$g(\Gamma) = -\frac{\alpha}{\beta}|\Gamma - \Gamma_0|^{\alpha-1}\text{sgn}(\Gamma - \Gamma_0)$$

so that our model (11) reduces to

$$\begin{cases} \dot{\Gamma} = \frac{4}{\mu+c-\frac{\alpha}{\beta}|\Gamma-\Gamma_0|^{\alpha-1}\text{sgn}(\Gamma-\Gamma_0)}\left(\frac{\Delta T-\Delta T_0}{2} + \frac{|\Gamma-\Gamma_0|^{\alpha}}{\beta}\right) \\ \Gamma(0) = 0. \end{cases} \tag{12}$$

From the mathematical theory of dynamical systems an explicit lower (i.e. conservative) estimate can be deduced for the lifetime of the material (see Appendix A):

$$\tilde{t} \geqslant \frac{\gamma_{opt}+1}{\gamma_{opt}}\frac{\pi(\mu+c)}{2\alpha\sin\frac{\pi}{\alpha}}\beta^{\frac{1}{\alpha}}\left(\frac{\Delta T-\Delta T_0}{2}\right)^{\frac{1-\alpha}{\alpha}} - \frac{\alpha}{4(\alpha-1)}\frac{1}{\gamma_{opt}-1} - \frac{\beta(\mu+c)}{4(\alpha-1)}\Gamma_0^{1-\alpha} \tag{13}$$

where γ_{opt} is given by

$$\gamma_{opt} = \frac{\pi\left(\frac{2}{\beta(\Delta T-\Delta T_0)}\right)^{\frac{\alpha-1}{\alpha}} + \sqrt{\pi\frac{\alpha^2}{\beta(\alpha-1)(\mu+c)}\left(\frac{2}{\beta(\Delta T-\Delta T_0)}\right)^{\frac{\alpha-1}{\alpha}}\sin\frac{\pi}{\alpha}}}{\pi\left(\frac{2}{\beta(\Delta T-\Delta T_0)}\right)^{\frac{\alpha-1}{\alpha}} - \frac{\alpha^2}{\beta(\alpha-1)(\mu+c)}\sin\frac{\pi}{\alpha}}. \tag{14}$$

In order to get some insight in this expression, we can consider its limit for great values of α, that is when the plateau of the saturation phase becomes flat. This corresponds to the setting of Morel's works (see [16,17]). Indeed, we obtain

$$\lim_{\alpha\to\infty}\gamma_{opt} = \frac{2+\sqrt{2\frac{\beta(\Delta T-\Delta T_0)}{\mu+c}}}{2-\frac{\Delta T-\Delta T_0}{\mu+c}} \approx 1$$

and

$$\lim_{\alpha\to\infty}\tilde{t} \geqslant \frac{\gamma_{opt}+1}{\gamma_{opt}}\frac{\mu+c}{\Delta T-\Delta T_0} - \frac{1}{4}\frac{1}{\gamma_{opt}-1} \approx \frac{2(\mu+c)}{\Delta T-\Delta T_0}$$

where the approximations at the end of the previous computations hold for small $\Delta T - \Delta T_0$. This estimate corresponds to [17, Equation (A9)].

Unfortunately, no simple and efficient expression could be derived for an analytical upper bound on the lifetime for our model.

5. Identification of the parameters from fatigue experiments

In the constitutive relation (9) for $G(\Gamma)$ and in Eq. (11), five different parameters appear: namely $\mu + c, \Delta T_0, \Gamma_0, \alpha$ and β. Moreover, since our model is essentially one-dimensional, ΔT has also to be evaluated starting from each 3D macroscopic loading state of interest.

In order to evaluate ΔT and ΔT_0 we adopt the same approach used by Morel in [16]. Starting from the Dang Van criterion (see [5,6]), we assume that the material undergoes elastic shakedown if

$$\Delta T + A S^H_{\max} \leqslant B,$$

where $S^H_{\max}$ is the maximum value reached by the mesoscopic (and macroscopic) hydrostatic stress during the periodic loading, while ΔT is a suitable measure of the resolved shear stress acting along the most solicited slip direction plane. In particular, we will use the following definition (see Morel [16] and Papadopoulos [22])

$$\Delta T = \max_{\theta,\phi} T_\sigma(\theta,\phi)$$

where

$$T_\sigma(\theta,\phi) = \sqrt{\int_0^{2\pi} T_a^2(\theta,\phi,\psi)\,\mathrm{d}\psi}.$$

Here θ and ϕ are angular variables used to identify the plane orthogonal to the versor

$$\mathbf{n} = \begin{pmatrix} \sin\theta\cos\phi \\ \sin\theta\sin\phi \\ \cos\theta \end{pmatrix},$$

in the physical space, ψ is an angle parametrizing all possible directions $\mathbf{m}$ in the slide plane identified by $\mathbf{n}$ and $T_a(\theta,\phi,\psi)$ is the amplitude of the variation of the mesoscopic resolved shear stress $\boldsymbol{\tau}$ defined above.

The material parameters A and B can be related to the fatigue limits under fully reversed tension compression f_{-1}, and under fully reversed torsion t_{-1}:

$$A = \frac{\sqrt{\pi}\left(t_{-1} - \frac{f_{-1}}{2}\right)}{\frac{f_{-1}}{3}}, \qquad B = \sqrt{\pi}\, t_{-1}.$$

In the simple case of sinusoidal loading, that is for loadings in the form

$$\boldsymbol{\Sigma} = \begin{pmatrix} \sigma^m_{xx} + \sigma^a_{xx}\sin(\omega t) & \tau^a_{xy}\sin(\omega t + \varphi) & 0 \\ \tau^a_{xy}\sin(\omega t + \varphi) & 0 & 0 \\ 0 & 0 & 0 \end{pmatrix} \tag{15}$$

for a suitable reference frame, where σ^m_{xx} is the mean normal stress in the x direction, σ^a_{xx} and τ^a_{xy} are the amplitude of the normal and shear stresses, ΔT and ΔT_0 can be explicitly computed and are given by the following expressions:

- In phase tension and torsion ($\varphi = 0^\circ$)

$$\Delta T_0 = \frac{t_{-1} f_{-1} - \left(t_{-1} - \frac{f_{-1}}{2}\right)\sigma^m_{xx}}{f_{-1} + \left(t_{-1} - \frac{f_{-1}}{2}\right)\frac{\sigma^a_{xx}}{\sqrt{\frac{(\sigma^a_{xx})^2}{4} + (\tau^a_{xy})^2}}}$$

$$\Delta T = \frac{t_{-1} f_{-1} - \left(t_{-1} - \frac{f_{-1}}{2}\right)\sigma^m_{xx}}{f_{-1}\left((\sigma^a_{xx})^2 + (\tau^a_{xy})^2\right) + 2\left(t_{-1} - \frac{f_{-1}}{2}\right)(\sigma^a_{xx})^2} \cdot \sqrt{\frac{(\sigma^a_{xx})^2 + (\tau^a_{xy})^2}{2}}\sqrt{(\sigma^a_{xx})^2 + (\tau^a_{xy})^2 + |(\sigma^a_{xx})^2 - 3(\tau^a_{xy})^2|}$$

- Out of phase tension and torsion ($\varphi = 90^\circ$)

$$\Delta T_0 = \sqrt{\frac{(\sigma^m_{xx})^2}{4} + (\tau^a_{xy})^2}$$

$$\Delta T = \frac{\sqrt{(\sigma^a_{xx})^2 + (\tau^a_{xx})^2}}{2\sqrt{2}\sigma^a_{xx}}\sqrt{(\sigma^a_{xx})^2 + (\tau^a_{xy})^2 + |(\sigma^a_{xx})^2 - 3(\tau^a_{xy})^2|}$$

We now consider the other modelling parameters. We observe that the kinematic hardening parameter c and the Lamè shear modulus μ may in principle be considered material constants already known from other experiments. However, in this work, we will identify them together with the other material constants appearing in (9) and (11): Γ_0, α and β. We note, moreover, that μ and c always appear together in the above expressions (in particular, see Eq. (11)) so that only a joint estimate of the sum $\mu + c$ can be obtained with this model. The identification of these four remaining parameters will be achieved through optimisation of a suitable cost function (see e.g. [13]). Two choices seem natural in this context:

- minimising the sum of the squared errors between the experimental lifetimes and the simulated ones;
- minimising the sum of the squared relative errors between the experimental lifetimes and the simulated ones.

These two approaches have led to very similar results in the experimental validation of our model of the next sections. Following [13], we will therefore report only the results using the first of the two approaches.

6. Results and discussion

In order to assess the efficiency of the estimate for the predicted lifetime obtained above, we compared the numerical solution of system (11) describing the evolution of the cumulated mesoscopic plastic strain, to the analytical approximation of lifetime given by estimates (13) and (14). The complete integration of (11) was performed using a high-order Runge–Kutta scheme (in particular a Runge Kutta (4,5) method was used—see [14, routine `ode45`]). We emphasise that the estimate (13) is a lower bound for the lifetime and therefore it is a theoretical conservative estimate.

On account of the many different tests done, we report in Fig. 6 the results of some numerical experiments showing a good agreement of approximation (13) for physically meaningful parameters, when the "flatness" parameter α is large enough. In order to assess the efficiency of the analytical approximation deduced previously, we introduce the following efficiency ratio

$$\eta = \frac{\text{lifetime given by (13)}}{\text{lifetime obtained by numerical integration of (12)}}.$$

We observe that values of η near 1 correspond to efficient estimates and that if $\eta < 1$ the analytical bound is conservative. In particular, as soon as α is greater than 4 or 5, the approximation is efficient for all the values of $\Delta T - \Delta T_0$, which arise in experiments and which can be accounted for with this kind of model (usually $\Delta T - \Delta T_0 \approx 10^0 \div 10^3 MPa$ for metallic materials). In order to keep the discussion as simple as possible, only integer values of α were considered here. However, α can be any real number greater than 1.

In Fig. 6 the behaviour of η with respect to the load $\Delta T - \Delta T_0$ is shown. The different lines correspond to the representative values for α, $\alpha = 2, 3, 4$ and 6. All other parameters are physically relevant and have been kept constant to ease comparison. In particular we have considered $\Gamma_0 = 66$, $\mu + c = 2{,}800{,}000$ MPa, $\beta = 70{,}000$ MPa^{-1} $\Delta T_0 = 445$ MPa. The horizontal line at height 1 represents a

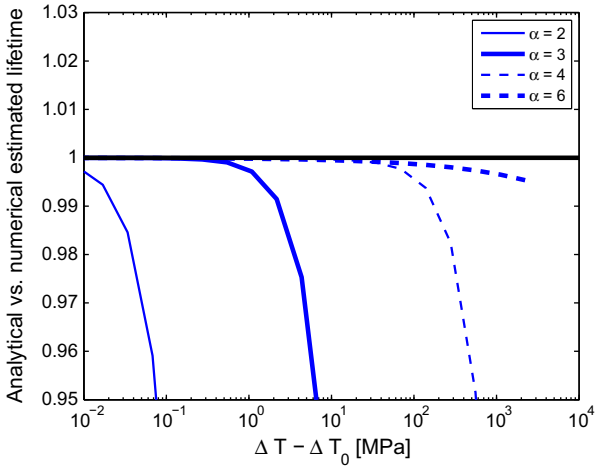

Fig. 6. The dependence of the efficiency ratio η (ratio between the analytical estimate (13) and the lifetime obtained by numerical integration of (12), see text) vs. the load $\Delta T - \Delta T_0$ for different values of the parameter α of the model. See text for description.

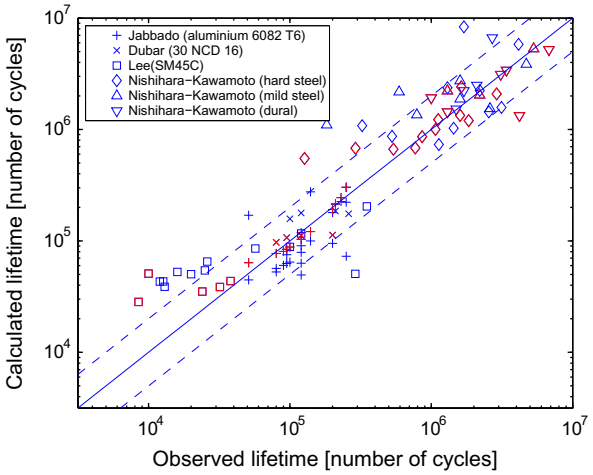

Fig. 7. The computed versus observed lifetimes from different fatigue tests. The data used to fit the model for each material are highlighted in red (training points) while the other observations used to check the validity of the approximation are in blue (control points). (For interpretation of the references to colour in this figure legend, the reader is referred to the web version of this article.)

perfect estimate. As expected, the analytical estimate derived above is confirmed to be conservative.

We have finally checked the effectiveness of our model in fitting experimental results and in predicting failure. To this end, we use some of the experimental data which can be found in the literature (see [8,11,12,18,20]). In each case, we have used the data coming from simple tension compression tests (called training points in the sequel) to fit the parameters of the model and to make predictions for the other observations. The results of these experiments (predicted endurance limit vs. experimental values) can be found in Fig. 7. Data used to fit the model (training points) are highlighted in red, while the remaining observation used to check the model (control points) are in blue. In this plot the diagonal represents perfect agreement between the model and the experimental values, whereas the two dashed limes represent a factor 2 acceptable tolerance.

As can be seen from Fig. 7, the agreement between estimated and observed lifetimes is quite satisfactory. Most of the experimental points fall between the two dashed tolerance lines for a wide range of the experimental parameters and a variety of materials considered. Scatter of experimental data up to 3–5 times that of the fatigue curve is indeed typical of HCF, which is due to individual properties of the material local zones. That is why scatter of data presented in Fig. 7 can be considered as regular if individual properties of the specimen are not taken into account.

7. Conclusions

We have proposed a new model for the lifetime of materials in the HCF regime. This model is a refinement of the one introduced by Morel in [17] based on the DVK criterion. In particular, it provides a more thorough understanding of the basic phenomena and gives an explanation of the long transient behaviour observed in material between the initial accommodation and the final breakdown (or crack initialisation).

Our approach allows us to consider a richer mesoscopic hardening rule than already done in the literature. As in [16,17] our model involves an initial hardening, a long saturation phase and a final softening leading to failure. The nonlinear power law proposed depends on five different parameters. The a priori analysis and the numerical tests reveal that the most relevant among the parameters is α, which describes the "flatness" of the hardening law. Moreover, α is directly related to the lifetime estimate (13). All the parameters of the mesoscopic model can be estimated using a simple and efficient least-square optimisation procedure. Nevertheless, study of the relations between more refined microscopic models and the parameters should be performed in the future.

The additional detail of description introduced has only a minor impact on the computational cost of the model. Indeed, when studying crack initiation problems, the main computational tasks are related to the solution of stresses and strains on the whole structure of interest. Therefore, any algebraic criterion for failure detection (in opposition to more complex local relations) is practically equivalent from the point of view of computational costs.

The lifetime estimates obtained account well for the experiments. The residual unpredicted variability is consistent with the usual scattering of HCF experimental data.

The main advantage of the proposed method based on dynamical systems techniques is the possibility of extending it to a large class of local material behaviour involving not only plasticity, but also crack and damage evolution, while keeping a simple closed-form formula for the prediction of the lifetime.

Finally we note that the extension of this approach to more complex periodic and quasi-periodic multiaxial loadings and to a larger base of materials constitute interesting fields of research, which are relevant for applications and which remain still largely unexplored.

Acknowledgments

The first author was partially supported by the French Embassy in Italy and by the "Bando Vinci 2011" Grant No. C2–95 issued by the Italian–French University (UIF–UIF). The authors want to thank the referee for his comments, which have greatly benefited this work.

Appendix A. A priori estimates

In this section we will derive the bound (13) and (14) for the dynamical system (12). In order to simplify the notation and focus on the main analytical argument, we will consider the following equivalent Cauchy problem

$$\begin{cases} \dot{y} = h(y) \doteq \frac{\epsilon + A|y|^{\alpha}}{1 - B|y|^{\alpha - 1} sgn y} \\ y(0) = y_0. \end{cases} \tag{A.1}$$

with $y_0 \leqslant 0$. We observe that all the results of this section can be readily adapted to our original model (12) by setting:

$$\epsilon = \frac{4}{\mu + c}\frac{\Delta T - \Delta T_0}{2}$$
$$A = \frac{4}{\mu + c}\frac{1}{\beta}$$
$$B = \frac{1}{\mu + c}\frac{\alpha}{\beta}$$
$$y_0 = -\Gamma_0.$$

We start by rigourously defining the lifetime for our system.

Definition 1. The lifetime for system (A.1) is the time t^{ξ}_{y0} that is necessary for any solution to travel from y_0 to ξ where ξ is the vertical asymptote of h given by the (unique) real root of

$$1 - B|\xi|^{\alpha-1} sgn\xi = 0.$$

Before stating the main estimate, we recall an elementary result, which will be very important in the following. (see [26, Exercise 4.3.10]).

Theorem 2. *The time required for a solution of the differential equation*

$$\dot{y} = \epsilon + Ay^{\alpha}$$

to go from $-\infty$ to $+\infty$ is given by

$$t^{+\infty}_{-\infty} = \frac{\pi}{\frac{\alpha}{2}\sin\frac{\pi}{\alpha}} A^{-\frac{1}{\alpha}} \epsilon^{\frac{1-\alpha}{\alpha}}.$$

Consider now Eq. (A.1). In order to estimate the lifetime from below (conservative estimate of the endurance of the material) we will consider the following approximation from above of h:

$$h(y) \leqslant \widetilde{h}(y) \doteq \begin{cases} \epsilon + A|y|^{\alpha} & \text{if } y \leqslant 0 \\ \gamma(\epsilon + A|y|^{\alpha}) & \text{if } 0 \leqslant y \leqslant x_1 \\ +\infty & \text{otherwise} \end{cases}$$

where x_1 is defined by:

$$\gamma(\epsilon + A|x_1|^{\alpha}) = h(x_1), \quad x_1 \in (0, \xi) \qquad \text{i.e} \quad x_1 = \left(\frac{\gamma - 1}{B\gamma}\right)^{\frac{1}{\alpha-1}} \tag{A.2}$$

and γ will be determined later. Since solutions of the dynamical system associated to $\widetilde{h}$ travel slower than those of (A.1), we immediately deduce that

$$t^{\xi}_{y_0} = t^0_{y_0} + t^{x_1}_0 + t^{\xi}_{x_1} \geqslant \tilde{t}^0_{y_0} + \tilde{t}^{x_1}_0$$

where with $\tilde{t}^b_a$ we denote the time required by a solution of the dynamical system

$$\dot{y} = \widetilde{h}(y)$$

to travel from a to b.

We start by estimating $\tilde{t}^0_{y_0}$, always from below. We consider the further approximation

$$\dot{y} = \widetilde{\widetilde{h}}_A(y) \doteq A|y|^{\alpha}. \tag{A.3}$$

Reasoning as above, we deduce

$$\tilde{t}^0_{y_0} = \tilde{t}^0_{-\infty} - \tilde{t}^{y_0}_{-\infty} \geqslant \tilde{t}^0_{-\infty} - \tilde{\tilde{t}}^{y_0}_{A^{-\infty}}$$

By symmetry, Theorem 2 implies (see Fig. A.1).

$$\tilde{t}^0_{-\infty} = \frac{\pi}{\alpha \sin\frac{\pi}{\alpha}} A^{-\frac{1}{\alpha}} \epsilon^{\frac{1-\alpha}{\alpha}}$$

whereas a direct integration of Eq. (A.3) gives

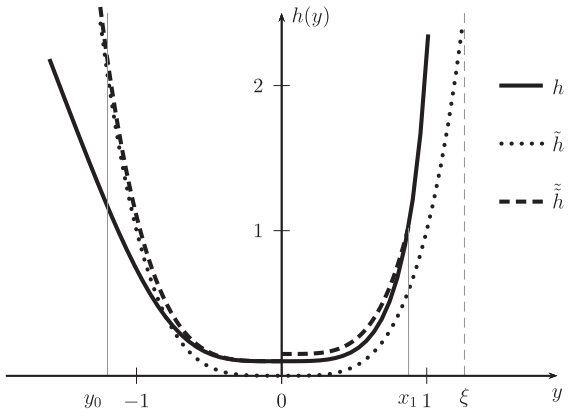

Fig. A.1. The approximations to the function $h(y)$ used in deriving the lower bound on the failure time for system (A.1).

$$\tilde{\tilde{t}}_{A^{y_0}_{-\infty}} = \frac{1}{A}\frac{1}{\alpha - 1}|y_0|^{1-\alpha}$$

from which we deduce

$$\tilde{t}^0_{y_0} \geqslant \frac{\pi}{\alpha \sin\frac{\pi}{\alpha}} A^{-\frac{1}{\alpha}} \epsilon^{\frac{1-\alpha}{\alpha}} - \frac{1}{A}\frac{1}{\alpha - 1}|y_0|^{1-\alpha}.$$

We now consider the lower approximation of the travelling time $\tilde{t}^{\xi}_0$ from 0 to ξ (failure). Arguing as before we deduce:

$$\tilde{t}^{\xi}_0 \geqslant \tilde{t}^{+\infty}_0 - \tilde{\tilde{t}}_{\gamma A^{+\infty}_{x_1}} = \frac{\pi}{\alpha\gamma \sin\frac{\pi}{\alpha}} A^{-\frac{1}{\alpha}} \epsilon^{\frac{1-\alpha}{\alpha}} - \frac{1}{\gamma A}\frac{1}{\alpha - 1} x_1^{1-\alpha}$$

Using the definition of x_1 given above (see (A.2)) we finally get

$$\tilde{t}^{\xi}_0 \geqslant \frac{\pi}{\alpha\gamma \sin\frac{\pi}{\alpha}} A^{-\frac{1}{\alpha}} \epsilon^{\frac{1-\alpha}{\alpha}} - \frac{B}{A(\alpha - 1)}\frac{1}{\gamma - 1}$$

which is minimised when

$$\gamma = \gamma_{opt} \doteq \frac{\pi\left(\frac{A}{\epsilon}\right)^{\frac{\alpha-1}{\alpha}} + \sqrt{\pi B \frac{\alpha}{\alpha-1}\left(\frac{A}{\epsilon}\right)^{\frac{\alpha-1}{\alpha}} \sin\frac{\pi}{\alpha}}}{\pi\left(\frac{A}{\epsilon}\right)^{\frac{\alpha-1}{\alpha}} - \frac{\alpha}{\alpha-1} B \sin\frac{\pi}{\alpha}}$$

for ϵ small enough.

Putting all the above results together we finally obtain the following estimate from below to the lifetime of our model:

$$t^{\xi}_{y_0} \geqslant \frac{\gamma_{opt} + 1}{\gamma_{opt}}\frac{\pi}{\alpha \sin\frac{\pi}{\alpha}} A^{-\frac{1}{\alpha}} \epsilon^{\frac{1-\alpha}{\alpha}} - \frac{B}{A(\alpha - 1)}\frac{1}{\gamma_{opt} - 1} - \frac{1}{A}\frac{1}{\alpha - 1}|y_0|^{1-\alpha}.$$

After substitution of the values for A, B, ϵ and y_0 arising in our model, we finally deduce the desired estimate on the lifetime.

References

[1] Bender CM, Orszag SA. Advanced mathematical methods for scientists and engineers. I. New York: Springer-Verlag; 1999 [Asymptotic methods and perturbation theory, Reprint of the 1978 original].
[2] Cano F, Constantinescu A, Maitournam H. Critère de fatigue polycyclique pour des matériaux anisotropes: application aux monocristaux. Comptes Rendus Mecanique 2004;332(2):115–21.
[3] Charkaluk E, Bignonnet A, Constantinescu A, Dang Van K. Fatigue design of structures under thermomechanical loadings. Fatigue & Fracture of Engineering Materials & Structures 2002;25(12):1199–206.
[4] Constantinescu A, Korsunsky A. Elasticity with mathematica. Cambridge University Press; 2007.
[5] Dang-Van K. Sur la résistance à la fatigue des métaux. Sciences Technique Armement 1973;47(3).
[6] Dang-Van K. Macro–micro approach in high-cycle multiaxial fatigue. ASTM Special Technical Publication, vol. 1191; 1993. p. 120.
[7] Dang-Van K. Introduction to fatigue analysis in mechanical design by the multiscale approach, pages 1691–1710. High-Cycle fatigue in the context of mechanical design, CISM courses and lectures, vol. 392. Springer-Verlag; 1999.
[8] Dubar L, et al. Fatigue multiaxiale des aciers. passage de l'endurance à l'endurance limitée. Prise en compte des accidents géométriques; 1992.

[9] Germain P. Mécanique des milieux continus. Paris: Masson; 1983.
[10] Guckenheimer J, Holmes P. Nonlinear oscillations, dynamical systems, and bifurcations of vector fields, applied mathematical sciences, vol. 42. New York: Springer-Verlag; 1990 [Revised and corrected reprint of the 1983 original].
[11] Jabbado M. Fatigue polycyclique des structures métalliques: durée de vie sous chargements variables. PhD thesis, Ecole Polytechnique; 2006.
[12] Lee SB. A criterion for fully reversed out-of-phase torsion and bending. In: ASTM; 1985. p. 553–68.
[13] Maitournam M, Krebs C, Galtier A. A multiscale fatigue life model for complex cyclic multiaxial loading. Int J Fatigue 2011;33:232–40.
[14] MATLAB. version 7.12.0 (R2011a). The MathWorks Inc., Natick, Massachusetts; 2011.
[15] Monchiet V, Charkaluk E, Kondo D. Plasticity-damage based micromechanical modelling in high cycle fatigue. Comptes Rendus Mecanique 2006;334(2):129–36.
[16] Morel F. A fatigue life prediction method based on a mesoscopic approach in constant amplitude multiaxial loading. Fatigue Fract Eng Mater Struct 1998;21(3):241–56.
[17] Morel F. A critical plane approach for life prediction of high cycle fatigue under multiaxial variable amplitude loading. Int J Fatigue 2000;22(2):101–19.
[18] Morel F, Petit J. Fatigue multiaxiale sous chargement d'amplitude variable. PhD thesis; 1996.
[19] Nguyen QS. On shakedown analysis in hardening plasticity. J Mech Phys Solids 2003;51(1):101–25.
[20] Nishihara T, Kawamoto M. The strength of metals under combined alternating bending and torsion with phase difference. Memor Coll Eng, Kyoto Imperial Univ 1945;11(85):112.
[21] Papadopoulos IV. Fatigue polycyclique des métaux: une nouvelle approche. PhD thesis, Ecole nationale des ponts et chaussées (France); 1987.
[22] Papadopoulos IV. Fatigue limit of metals under multiaxial stress conditions: the microscopic approach. ISEI: Joint Research Centre; 1993.
[23] Papadopoulos IV. A high-cycle fatigue criterion applied in biaxial and triaxial out-of-phase stress conditions. Fatigue Fract Eng Mater Struct 1995;18(1):79–91.
[24] Papadopoulos IV. Critical plane approaches in high-cycle fatigue: on the definition of the amplitude and mean value of the shear stress acting on the critical plane. Fatigue Fract Eng Mater Struct 1998;21(3):269–85.
[25] Papadopoulos IV, Davoli P, Gorla C, Filippini M, Bernasconi A. A comparative study of multiaxial high-cycle fatigue criteria for metals. Int J Fatigue 1997;19(3):219–35.
[26] Strogatz SH. Nonlinear dynamics and chaos. MA: Addison-Wesley Reading; 1994.